

Brief/Technical Note

Measuring Surface Roughness of Pharmaceutical Powders Using Vapor Sorption Methods

Daniel J. Burnett,^{1,5} Jerry Y. Y. Heng,² Frank Thielmann,³ Armando R. Garcia,¹ Majid Naderi,⁴ and Manaswini Acharya⁴

Received 5 August 2010; accepted 8 December 2010; published online 18 December 2010

KEY WORDS: dry powder formulations; dynamic vapor sorption; surface profilometry; surface roughness.

INTRODUCTION

Particle morphology of pharmaceutical solids has practical importance for several reasons. In particular, surface roughness can influence formulation development and pharmaceutical performance for a wide range of delivery types including oral tablets and dry powder formulations for inhalation. For instance, the surface roughness can influence dissolution, friability, and adhesion of coatings and films for bare tablets (1–5). To illustrate, surface roughness correlated strongly with tablet friability for erythromycin acistrate tablets (3). The surface roughness has also been related to gloss and permeability, such that the reflectivity and surface texture of coated tablets were directly correlated (6,7). The surface roughness of particles also has been correlated to powder flow and powder packing (8), where the smoother particles led to an improvement of powder packing and flow properties.

The adhesion of particles to surfaces or other particles can also be greatly affected by surface roughness. This is of particular concern for dry powder inhalation (DPI) formulation development. Dry powder formulations are often composed of small drug particles and inert larger carrier particles. Interactions between these particles can be dominated by physico-chemical properties of the particle, such as size, shape, morphology, contact area, and hygroscopicity (9,10). In particular, it has been shown that the surface roughness of the carrier particles has a significant impact on the adhesion and friction forces between the carrier and drug particles (11,12). Adhesion, blend homogeneity, and stability

have been directly related to the surface roughness of the carrier particle (13). The ultimate performance properties of DPI blends as determined by *in vitro* testing has also been correlated to the primary particle surface roughness (13–15).

There is an important balance between the relative scaling in the roughness of the particles and the relative size of the carrier and drug particles when considering the effects of surface roughness on particle–particle adhesion. This was previously described (16) and is illustrated by the schematic in Fig. 1. Assuming no other changes in particle properties (*i.e.*, surface energy, particle size, amorphous content, hygroscopicity, etc.), the rank order of drug-carrier adhesion would obey the following trend in roughness of the larger carrier particle: macro-rough surface (Fig. 1a) > smooth surface (Fig. 1b) > micro-rough surface (Fig. 1c). This trend is strictly dependent on the contact area between drug and carrier. If adhesion is too weak, the active drug may be released during inhalation before the particles reach the deep lung. On the contrary, if adhesion is too strong, the active may not be released at all. This phenomenon has been observed and described in detail for several DPI studies (15–19).

In this study, we focus on the measurement of micro-scale roughness using fractal dimensions determined from sorption isotherms with different adsorbates.

MATERIALS AND METHODS

Samples

Alumina powder (Al₂O₃; CRM 171; Community Bureau of Reference; Brussels, Belgium) was chosen as a model inorganic material. This sample was milled using a bench-top, high-speed grinder for 30 min (Cuisinart, model DGC-20). Microcrystalline cellulose (MCC; Avicel® PH101, FMC) was chosen as a model pharmaceutical excipient. The MCC sample was milled for 5 min. Both the milled and as-received (unmilled) samples were sieved to less than 63 μm (230-mesh) in order to minimize any particle size dependence on the

¹Surface Measurement Systems Ltd, 2125 28th Street SW, Suite 1, Allentown, Pennsylvania 18103, USA.

²Department of Chemical Engineering, Imperial College London, London, UK.

³Novartis Horsham Research Centre, West Sussex, UK.

⁴Surface Measurement Systems, Alpertown, UK.

⁵To whom correspondence should be addressed. (e-mail: burnett@smsna.com)

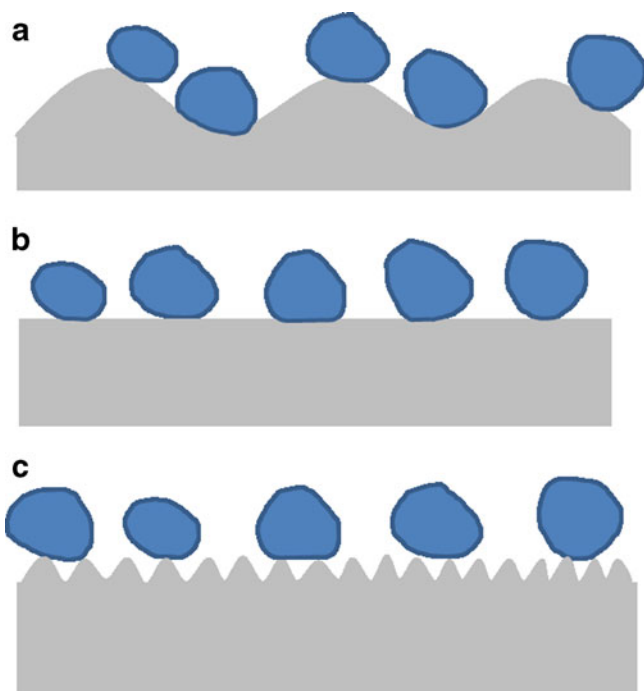


Fig. 1. Illustration of macro-roughness (a), smooth surface (b), and micro-roughness (c) affects on particle-particle contact and adhesion

results. Micronized budesonide (BU) and beclomethasone dipropionate (BDP) were provided by Novartis Pharmaceuticals (Basel, Switzerland) and used as is.

Particle Size

Particle size distributions were measured using a Malvern Mastersizer 2000 (Malvern, UK). Water was used as the dispersant. A size range of 0.020 to 2000.000 μm was used.

Fractal Dimensions

This study utilizes an approach that is based on the sorption behavior of different-sized adsorbates (20–23). This method is based on measuring the monolayer coverages for a range of adsorbates with different molecular sizes to determine the surface fractal dimension (D value). The pioneering

work in this field was carried out by Anvir and Pfeifer (20,24), who showed that the volume of molecules required to cover the surface with a monolayer (V_{mono}) is given by

$$V_{\text{mono}} = S\sigma \frac{-D}{2} \quad (1)$$

where S is the Hausdorff measure of the surface and σ is the effective cross-sectional area of the adsorbate. For a Euclidean, perfectly smooth surface, $D=2$ and S is the surface area. The value of D increases with the degree of surface irregularity, and for very rough, irregular surface, the value of D approaches 3. As can be seen in Eq. 1, the monolayer volume decreases with the cross-sectional area of the adsorbate more rapidly for a rough surface compared with a smooth surface. From Eq. 1 the following is derived:

$$\ln(V_{\text{mono}}) = \ln(S) - \frac{D}{2} \ln(\sigma) \quad (2)$$

By changing the size of the adsorbate and by determining the corresponding monolayer content of the surface, the surface fractal dimension can be found from a plot of $\ln(V_{\text{mono}})$ versus $\ln(\sigma)$, where D is equal to -2 times the resulting slope.

In this study, dynamic gravimetric vapor sorption (DVS) was used to determine the surface fractal dimensions. Gravimetric vapor sorption experiments were undertaken using the DVS-Advantage-1 instrument (Surface Measurement Systems, London, UK). Samples (~ 100 mg) were placed into the instrument at $25.0 \pm 0.2^\circ\text{C}$ where they were initially dried in a 100 sccm (standard cubic centimeters per minute) stream of dry air for several hours to establish a dry mass. The samples were then exposed to the desired vapor partial pressure profile while monitoring the sample mass. Sorption isotherms and subsequent monolayer coverages were determined for a range of n -alkane adsorbates using the Brunauer–Emmett–Teller (BET) equation (25). The BET isotherm equation is a widely used model for surface sorption isotherms between 0.05 and 0.40 relative vapor pressure. It provides an estimate of monolayer value of vapor adsorbed on the surface. Equation 3 displays the BET equation where x is the relative pressure of the vapor above the solid surface, V is the amount of vapor sorbed, V_m is the amount of gas sorbed if a monolayer were to form, and c is a

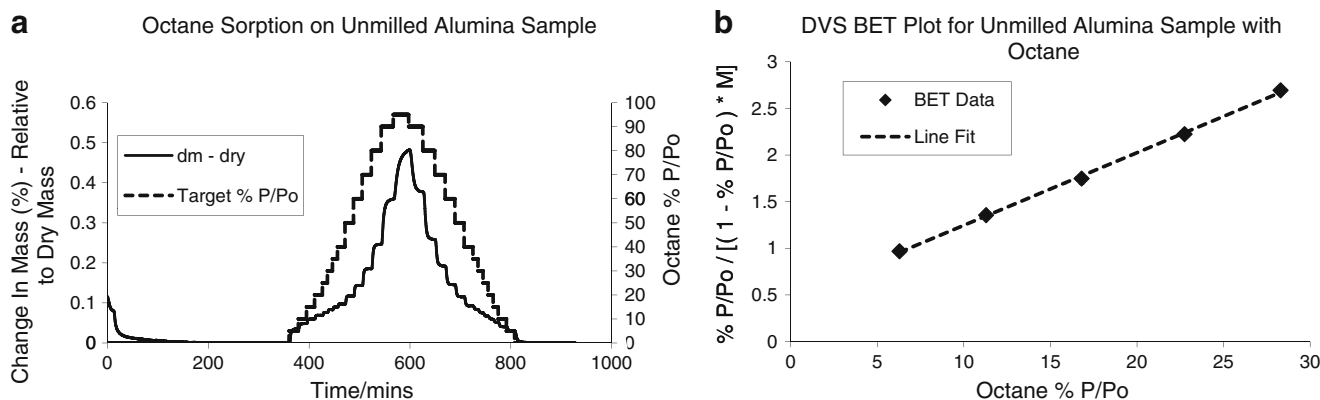


Fig. 2. Octane vapor sorption profile (a) and resulting BET plot (b) for unmilled Alumina sample at 25°C

Table I. Monolayer Volumes Determined Using BET Equation for *n*-Alkanes on Unmilled Alumina, Milled Alumina, Unmilled MCC, Milled MCC, BU, and BDP Samples

Adsorbate	Cross-sectional area (Å ²)	Monolayer volume (cm ³ /g), unmilled alumina	Monolayer volume (cm ³ /g), milled alumina	Monolayer volume (cm ³ /g), unmilled MCC	Monolayer volume (cm ³ /g), milled MCC	Monolayer volume (cm ³ /g), BU	Monolayer volume (cm ³ /g), BDP
Hexane	51.5	0.1523	0.1869	–	0.1039	0.1146	0.0644
Heptane	57.3	0.1385	0.1661	0.115	0.1227	0.1023	0.0575
Octane	63.0	0.1211	0.1404	0.1002	0.1005	0.0909	0.0487
Nonane	69.0	0.1120	0.1248	0.08974	0.09026	–	0.0440
Decane	75.0	0.1033	0.1104	0.08238	0.08139	–	–

MCC microcrystalline cellulose, BU budesonide, BDP beclomethasone dipropionate

constant related to the adsorbate–adsorbent strength of interaction. A plot of $(1/V)[x/(1-x)]$ versus x should yield a straight line, where the gradient yields V_m and c is the intercept.

$$\frac{1}{V} \frac{x}{1-x} = \frac{c-1}{cV_m} x + \frac{1}{cV_m} \quad (3)$$

The BET equation assumes a physical adsorption mechanism in which monolayer coverage is obtained, followed by multilayer adsorption.

To the authors' knowledge, this is the first report to measure surface fractal dimensions using the gravimetric vapor sorption technique. All previous studies have used volumetric sorption techniques.

Surface Profilometry

Optical Profilometry (Veeco Wyko NT9100, Plainview, NY) was conducted using the vertical scanning interferometry mode, and each scan was carried out at full resolution using a $\times 50$ Mirau objective lens with a $\times 2.0$ field of view lens giving an effective magnification of $\times 98.8$. Primary scan parameters were set at 0 mm backscan, 75 mm scan length, $1\times$ scan speed, and 1% modulation threshold. Post-scan analysis was conducted using the multi-region analysis as part of the operating software (VISION 4.10 Update 3) to give the common roughness amplitude parameters. In this study, the root mean square measurement of the surface roughness amplitude values, R_q , were used as a measure of surface roughness.

RESULTS

Particle Size

For the unmilled (as-received) alumina sample, the $d(0.1)$, $d(0.5)$, and $d(0.9)$ values were 1.08, 2.70, and 8.83 μm . Likewise, for the milled alumina sample the values were 1.19, 2.83, and 9.45 μm .

For the unmilled MCC sample, the $d(0.1)$, $d(0.5)$, and $d(0.9)$ values were 23.32, 64.17, and 129.23 μm , respectively. Similarly, for the milled MCC sample, the $d(0.1)$, $d(0.5)$, and $d(0.9)$ values were 19.65, 52.92, and 107.12 μm . The MCC samples were physically sieved using a 230-mesh screen such that all particles were expected to be smaller than 63 μm . As the $d(0.5)$ and $d(0.9)$ values indicate, there is a significant portion of particles larger than 63 μm , as measured by the laser diffraction. The type of MCC used was Avicel PH 101, which has been reported to have rod-like particles (26). Therefore, it is possible that particles were able to go through the mesh through the short axis and be measured by laser diffraction (which assumes spherical particles) based on their long axis. The particle size values for the milled MCC sample are slightly lower for the unmilled MCC sample ($\sim 15\%$ smaller particles). Despite these small differences, the particle size distributions are quite similar for the two samples, and differences measured in surface roughness are not expected to be an artifact of different particle sizes.

Fractal Dimensions

Figure 2a shows the octane sorption and desorption kinetics for the unmilled alumina sample at 25°C. Note that equilibrium has been reached at each vapor pressure step.

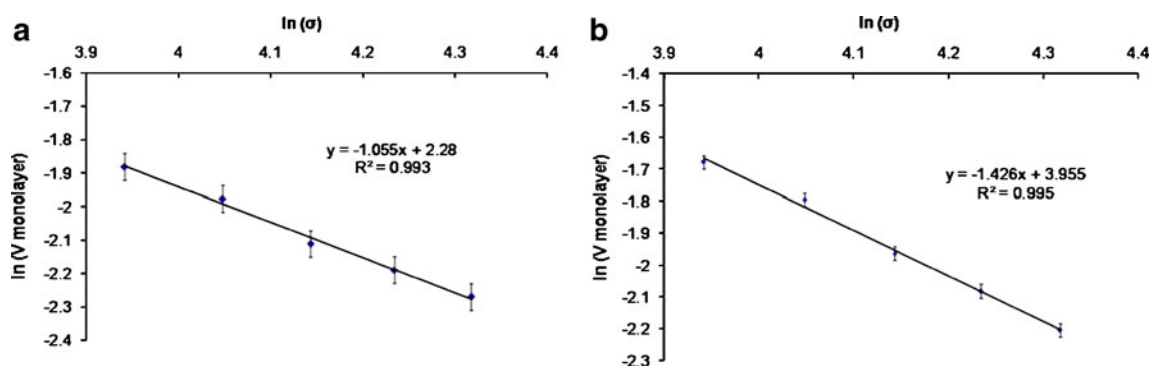


Fig. 3. Fractal dimension plots for unmilled (a) and milled (b) alumina samples

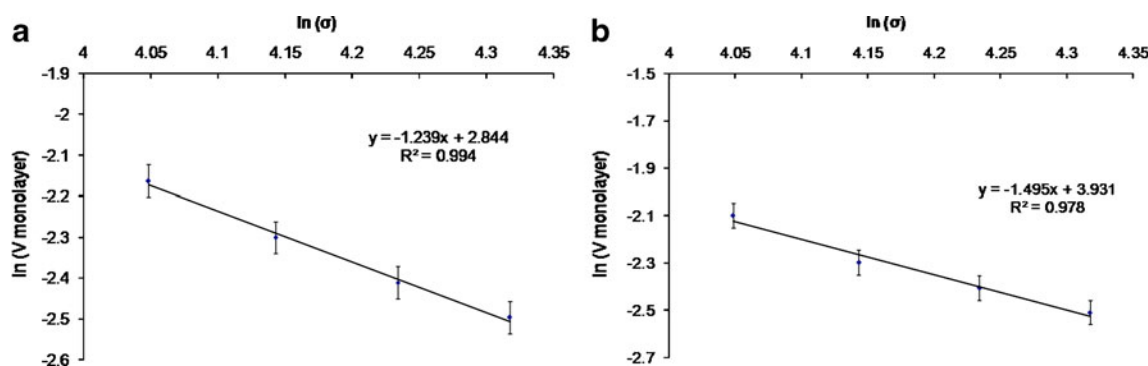


Fig. 4. Fractal dimension plots for unmilled (a) and milled (b) MCC samples (sieved below 63 μm)

From the equilibrium mass uptakes at each vapor pressure, the sorption isotherm was determined and used for the BET analysis. Figure 2b shows the resulting BET plot and fit for this sample. Figure 2a, b is representative for all sorption measurements and BET calculations. Table I displays the average monolayer coverage values ($n=3$) obtained using the BET calculation (Eq. 3) and cross-sectional areas for the different vapors measured on the unmilled and milled alumina samples. Using Eq. 2, the slopes in Fig. 3a, b were used to determine surface fractal roughness values of 2.11 and 2.85 for the unmilled and milled alumina samples, respectively. Error bars in Fig. 3a, b represent the first standard deviation for the monolayer coverages based on three measurements.

Table I also displays the average ($n=3$) monolayer coverage values and corresponding cross-sectional areas for the various probe molecules measured on the milled and unmilled MCC samples (sieved below 63 μm). The resulting plots are shown in Fig. 4a (unmilled) and Fig. 4b (milled). The vertical error bars represent the first standard deviation in the measured monolayer coverage values ($n=3$). Milling increased the fractal dimension from 2.48 to 2.99.

The measured alkane monolayer volumes for the BU and BDP samples are shown in Table I. The fractal dimension plots are shown in Fig. 5a (BDP) and Fig. 5b(BU), resulting in values of 2.67 and 2.29, respectively.

Surface Profilometry

Surface profilometry experiments were only performed on the MCC samples. The focus of this paper was measuring surface roughness via sorption techniques. Measurements on

20 separate particles resulted in an average Rq value of 4.24 μm (1.56 μm SD) for the unmilled MCC sample and an average Rq value of 5.91 μm (2.43 μm SD) for the milled MCC sample. Despite the small differences and high standard deviations, a single-factor ANOVA test, these differences are statistically significant (p value of 0.018 using 95% confidence limits).

DISCUSSION

The alumina sample was used as a model inorganic material. Due to its hardness, alumina is often used as an abrasive or grinding material. The particle size measurements confirmed that milling did not significantly alter the particle size of the alumina powders. This is expected due to the structurally robust nature of this alumina sample. However, milling did have a measurable effect on surface roughness as measured by the gravimetric vapor sorption technique. The fractal dimension increased from 2.11 to 2.85. The surface fractal dimension values are measurements of surface roughness on the same order as the adsorbates' cross-sectional areas used. For this study, the adsorbates had molecular cross-sectional areas between 51.5 and 75.0 \AA^2 . Therefore, the resulting fractal dimensions can be considered to be a measure of micro-roughness. Despite the robust nature of alumina and no significant changes in particle size, milling does affect the surface topography on the same order of magnitude as the molecular probes. This could be due to small dislocations on the surface or the introduction of defect sites. This could lead to very small fragments or chips being removed during milling, but these were not detectable in the particle size analysis.

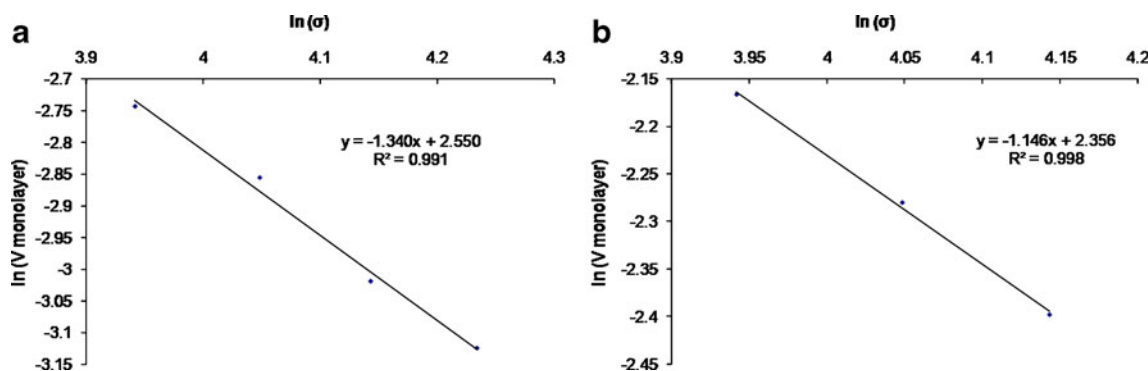


Fig. 5. Fractal dimension plots for micronized BDP (a) and micronized BU (b) samples

For the MCC samples, milling increased both the macro-roughness and micro-roughness. The macro-roughness using optical profilometry showed a small but statistically significant increase in roughness (1.56 to 2.43 μm). Since measurements were measured on individual particles, it is important to sample enough particles to get a representative value of roughness using this technique. In this study, the values presented were based on the average of measurements on 20 particles. The micro-roughness measured using vapor sorption methods showed a more significant increase (2.48 to 2.99). In comparison to the surface profilometry technique, the vapor sorption approach accesses the entire surface of the powder used, thus averaging the interactions over a more representative sample. Also, the DVS technique would not have any particle size limitations that might be the case for other methods. To illustrate, optical profilometry may bias larger samples, as very small particles may not be readily detected and measured. The limitations would be down to the optical resolution. Since DVS accesses the entire exposed surface, both large particles and small particles are measured equally.

Milling could induce other surface changes (in addition to increasing surface roughness), such as, exposing different surface groups, fracturing different crystal planes, or introduce defect or other high-energy sites. All of these events could increase interactions with an individual vapor and increase its monolayer coverage. However, this would occur similarly for all probes, and the slopes generated from Eq. 1 would be unchanged. Milling may also be changing the surface chemistry, but this alone would not account for the change in fractal dimension.

For the model drug samples, the BDP sample had a higher micro-roughness value (2.67) compared with the BU sample (2.29). Therefore, if all other factors were similar (*i.e.*, same carrier molecule, particle size, surface energy, amorphous content, etc.), the BDP sample may have a weaker attachment and easier release from the carrier particle.

In this paper, we have demonstrated the use of gravimetric vapor sorption as means to measure surface roughness via surface fractal determination. Previous sorption studies using fractal dimensions have used volumetric techniques. Volumetric sorption techniques are often performed under low-pressure environments and/or sub-ambient temperatures. For some fragile organic solids, low pressure or low temperature conditions can cause structure collapse or agglomeration of small particles. For instance, primary and secondary particles of aluminum hydroxide adjuvant irreversibly agglomerate when dried under vacuum (27). Gravimetric techniques in this paper have the advantage that they were run at atmospheric pressure and room temperature. Also, volumetric techniques are typically static sorption techniques where equilibrium is achieved much slower than the dynamic gravimetric technique used in this paper.

Ultimately, the reliability and sensitivity of the fractal dimensions measured is reliant on the quality of the BET plots obtained and using as wide a range of adsorbate cross-sectional areas as possible. Since gravimetric vapor sorption methods have been reliable for determining BET surface area values (27,28), the gravimetric technique is expected to be as sensitive and reliable as volumetric techniques, provided the measurement conditions do not affect the sample properties as discussed above.

CONCLUSIONS

Surface profilometry and gravimetric vapor sorption techniques for measuring surface roughness have been performed on model inorganic, excipient, and drug substances. Vapor sorption measurements proved to be a reliable method to measuring micro-roughness for a wide range of materials. Gravimetric vapor sorption measurement of fractal surface roughness may be more advantageous than traditional volumetric techniques for fragile, organic solids. The surface profilometry experiments are a measure of macro-roughness on individual particles. Combined, these techniques allow for a greater understanding of the particle surface roughness. Changes in either macro- and micro-roughness can have a significant impact on pharmaceutical formulation development.

REFERENCES

1. Healy AM, Corrigan OI, Allan JEM. The effect of dissolution on the surface texture of model solid-dosage forms as assessed by non-contact laser profilometry. *Pharm Technol Eur.* 1995;9:14–22.
2. Podczec F. Measurement of surface roughness of tablets made from polyethylene glycol powders of various molecular weight. *Pharm Pharmacol Commun.* 1998;4:179–82.
3. Riipi M, Antikainen O, Niskanen T, Yliruusi J. The effect of compression force on surface structure, crushing strength, friability and disintegration time of erythromycin acistrate tablets. *Eur J Pharm Biopharm.* 1998;46:339–45.
4. Felton L, McGinity JW. Adhesion of polymeric films to pharmaceutical solids. *Eur J Pharm Biopharm.* 1999;47:3–14.
5. Missaghi S, Fassihi R. A novel approach in the assessment of polymeric film formation and film adhesion on different pharmaceutical solid substrates. *AAPS PharmSciTech.* 2004;5:E29.
6. Reiland TL, Eber AC. Aqueous gloss solutions: formula and process variables effects on the surface texture of film coated tablets. *Drug Dev Ind Pharm.* 1986;12:213–45.
7. Rohera BD, Parikh NH. Influence of plasticizer type and coat level on Surelease film properties. *Pharm Dev Technol.* 2002;7:407–20.
8. Ferrair F, Cocconi D, Bettini R, Giordano F, Santi P, Tobyn M, Price R, Young P, Caramella C, and Colombo P (2004) The surface roughness of lactose particles can be modulated by wet-smoothing using a high-shear mixer. *AAPS PharmSciTech.* 5: Article 60
9. Bell J (1994) Dry powder inhalation technology. *Pharm. Manufact. Int.* 179–182
10. Prime D, Atkins PJ, Slater A, Sumby B. Review of dry powder inhalers. *Adv Drug Deliv Rev.* 1997;26:51–8.
11. Podczec F. The relationship between particulate properties of carrier materials and the adhesion force of drug particles in interactive powder mixtures. *J Adhes Sci Technol.* 1997;11:1089–104.
12. Podczec F. Adhesion forces in interactive powder mixtures of a micronized drug and carrier particles of various particle size distributions. *J Adhes Sci Technol.* 1998;12:1323–39.
13. Flament M-P, Leterme P, Gayot A. The influence of carrier roughness on adhesion, content uniformity and the *in vitro* deposition of terbutaline sulphate from dry powder inhalers. *Int J Pharm.* 2004;275:201–9.
14. Podczec F. The influence of particle size distribution and surface roughness of carrier particles on the *in vitro* properties of dry powder inhalations. *Aerosol Sci Technol.* 1999;31:301–21.
15. Iida K, Hayakawa Y, Okomoto H, Danjo K, Leunberger H. Effect of surface layering time of lactose carrier particles on dry powder inhalation properties of salbutamol sulfate. *Chem Pharm Bull.* 2004;52:350–3.
16. Kawashima Y, Serigano T, Hino T, Yamamoto H, Takeuchi H. Effect of surface morphology of carrier lactose on dry powder

- inhalation property of pranlukast hydrate. *Int J Pharm.* 1998;172:179–88.
17. Young PM, Cocconi D, Colombo P, Bettini R, Price R, Steele DF, *et al.* Characterization of a surface modified dry powder inhalation carrier prepared by 'particle smoothing'. *J Pharm Pharmacol.* 2002;54:1339–44.
 18. Iida K, Inagaki Y, Todo H, Okamoto H, Danjo K, Leunberger H. Effects of surface processing of lactose carrier particles on dry powder inhalation properties of salbutamol sulfate. *Chem Pharm Bull.* 2004;52:938–42.
 19. Orafai H, Spring M. Roughness model for adhesion testing of pharmaceutical coating materials. *Iran J Basic Med Sciences.* 2007;10:124–31.
 20. Avnir D, Farin D, Pfeifer P. Molecular fractal surfaces. *Nature.* 1984;308:261–3.
 21. Suzuki T, Yano T. Fractal structure analysis of some food materials. *Agric Biol Chem.* 1990;54(12):3131–5.
 22. Kaneko K, Sato M, Suzuki T, Fujiwara Y, Nishikawa K, Jaroniec M. Surface fractal dimension of microporous carbon fibres by nitrogen adsorption. *J Chem Soc Faraday Trans.* 1991;87(1):179–84.
 23. Pettit FK, Bowie JU. Protein surface roughness and small molecular binding sites. *J Mol Biol.* 1999;285:1377–82.
 24. Pfeifer P, Avnir D. Chemistry in noninteger dimensions between two and three. I. Fractal theory of heterogeneous surfaces. *J Chem Phys.* 1983;79:3558–65.
 25. Brunauer S, Emmett PH, Teller E. Adsorption of gases in multimolecular layers. *J Am Chem Soc.* 1938;60:309–19.
 26. Zhang Y, Law Y, Chakrabarti S (2003) Physical properties and compact analysis of commonly used direct compression binders. *AAPS PharmSciTech.* 4:Article 62.
 27. Johnston CT, Wang S-L, Hem SL. Measuring the surface area of aluminum hydroxide adjuvant. *J Pharm Sci.* 2002;91(7):1702–6.
 28. Chlou CT, Rutherford DW. Sorption of N₂ and EGME vapors on some soils, clays, and mineral oxides and determination of sample surface areas by use of sorption data. *Environ Sci Technol.* 1993;27(8):1587–94.